Journal of Magnetic Resonance 286 (2018) 78–81

Contents lists available at ScienceDirect

Journal of Magnetic Resonance

journal homepage: www.elsevier.com/locate/jmr

Experimental investigation of a metasurface resonator for *in vivo* imaging at 1.5 T

Alena V. Shchelokova [a], Alexey P. Slobozhanyuk [a,b], Paul de Bruin [c], Irena Zivkovic [c], Efthymios Kallos [d], Pavel A. Belov [a], Andrew Webb [c,*]

[a] Department of Nanophotonics and Metamaterials, ITMO University, Saint Petersburg, Russian Federation
[b] Nonlinear Physics Center, Australian National University, Canberra, ACT 2601, Australia
[c] C.J. Gorter Center for High Field MRI, Department of Radiology, Leiden University, Medical Center, Leiden, The Netherlands
[d] MediWise | Medical Wireless Sensing Ltd, Queen Mary Bio Enterprise, London, UK

ARTICLE INFO

Article history:
Received 17 September 2017
Revised 18 November 2017
Accepted 21 November 2017
Available online 22 November 2017

Keywords:
Metasurface
Transmit efficiency
Specific absorption rate
Implant

ABSTRACT

In this work, we experimentally demonstrate an increase in the local transmit efficiency of a 1.5 T MRI scanner by using a metasurface formed by an array of brass wires embedded in a high permittivity low loss medium. Placement of such a structure inside the scanner results in strong coupling of the radiofrequency field produced by the body coil with the lowest frequency electromagnetic eigenmode of the metasurface. This leads to spatial redistribution of the near fields with enhancement of the local magnetic field and an increase in the transmit efficiency per square root maximum specific absorption rate in the region-of-interest. We have investigated this structure *in vivo* and achieved a factor of 3.3 enhancement in the local radiofrequency transmit efficiency.

1. Introduction

Nazarian et al. [1] have reported that the likelihood of a patient with an implanted medical device requiring an MRI scan is more than 75%. Clinical scans performed either at 1.5 T or 3 T normally use the body coil for radiofrequency (RF) transmission, meaning that RF is deposited in all parts of the body, not only in the region-of-interest. The presence of medical implants often results in scans with low specific absorption rate (SAR) being prescribed, which reduces the diagnostic quality of the images. In many cases a patient who would be scanned at 3 T in the absence of an implant is moved to a 1.5 T system since the power deposited in the patient is lower: again this process is accompanied by lower image quality.

In many cases the imaging region-of-interest is different from the area in which the medical device is implanted, or in which electrical leads to the medical device are located. In these cases the SAR issues can potentially be overcome if a local transmit coil rather than the body coil could be used. However, with a few exceptions (e.g. head and knee) there are very few local transmit coils which are produced commercially, and many sites do not have even those which are commercially available. To address this issue Yu et al. [2] proposed an elegant approach in which high permittivity materials [3,4] could be placed around the imaging region-of-interest in order to concentrate the local transmit field produced by the body coil, resulting in a reduction in the required power transmitted by the body coil for a given image contrast, and an associated reduction in global and local SAR [2]. The authors showed electromagnetic simulations at 3 T which suggested that judicious placement of such materials could result in a reduction of the SAR averaged over 1 g of tissue next to a pacemaker lead by almost 75%. This approach could potentially be extended to 1.5 T, although one would require materials with much higher permittivity values.

A potential alternative approach is to use metamaterial-like structures [5,6]. Some approaches to shaping the local magnetic fields using metamaterials for MRI have already been discussed in the literature [7–13]. For example, metamaterials made from split-ring resonators can be employed as matching devices between a patient and the receive coils and for local transmit efficiency improvement [9]. However, these types of structures are very complicated to construct and fine-tune. Recently, a simple two-dimensional structured metasurface has been proposed [11]. Results in phantoms showed that this artificial structure could effectively increase the local RF magnetic field at 1.5 T. However, in this original work, the geometry was not practical in requiring the sample to be placed in a high dielectric material and no

* Corresponding author at: C.J. Gorter Center for High Field MRI, Department of Radiology, Leiden University Medical Center, Albinusdreef 2, 2333 ZA Leiden, The Netherlands.
E-mail address: a.webb@lumc.nl (A. Webb).

https://doi.org/10.1016/j.jmr.2017.11.013
1090-7807/

detailed consideration of SAR was covered, which is a key element in translating its use to human scanning. In this current work we extend the principles developed for the original metasurface [11] and show the first human MRI scans at 1.5 T. An increase in the transmit field efficiency of up to a factor of 3.3 has been achieved, with a reduction in global SAR by the equivalent amount.

2. Methods

2.1. Electromagnetic simulations

For comparison between simulation and experimental results, a numerical model of the metasurface was developed in commercially available software (CST Microwave Studio 2016). A 16 rung high-pass birdcage coil (inner diameter 68 cm; length 104 cm) was used, loaded with the virtual voxel human model "Gustav" (from the CST voxel family) with a mesh resolution 2.08 × 2.08 × 2 mm^3. The B_1^+ field and SAR were calculated using the time domain solver. For phantom simulations the following parameters were used: $\varepsilon = 80 + 0.2i$ – low loss phantom, $\varepsilon = 80 + 168.5i$ – phantom with losses approximating those of the body; length 16 cm, width 6 cm and height 3 cm. The phantom was placed on top of the metasurface. Simulated effects of loading were evaluated using a model incorporating an untuned 4 cm diameter conducting loop placed directly below the center of the metasurface.

2.2. Experimental setup

All MR images were acquired on a Philips Ingenia 1.5 T system (Leiden University Medical Center, Leiden, The Netherlands). Volunteer experiments were approved by the local medical ethics committee. As described previously [11], the metasurface was assembled from an array of 14 × 2 brass wires with length L = 37 .2 cm, radius r = 0.1 cm, and period a = 1 cm which was placed in thin hollow 3D-printed ABS plastic holders and embedded in a watertight and mechanically robust box made of 0.5 cm thick acrylic sheet of dimensions 42.2 × 18.2 × 5.7 cm^3 filled with water ($\varepsilon = 80 + 0.2i$ at room temperature). The resonant frequency of the metasurface eigenmode characterized by the highest penetration depth was measured using a pick-up loop and vector network analyzer both outside and inside the magnet: minimal detuning was measured inside the bore. *In vivo* images were acquired using two multislice low tip angle T_1-weighted gradient echo sequences: (1) used for acquiring slices which cover both wrists (and abdomen), tip angle = 10^0, TR = 216 ms, TE = 3 ms, acquisition matrix = 280 × 280, field-of-view = 560 × 560 mm^2, acquisition time = 9 3 s; (2) used for zoomed imaging of one wrist placed above the metasurface: tip angle = 10^0, TR = 616.3 ms, TE = 18 ms, acquisition matrix = 120 × 120, field-of-view = 120 × 120 mm^2, acquisition ti me = 101 s. The transmit efficiency (B_1^+ per square root input power) was calculated using a single image acquired using the larger field-of-view obtained with the body coil in transmit and receive mode and the metasurface placed underneath one wrist of the volunteer, while the other wrist was located on top of a sandbag. The signal intensities in each wrist are proportional to the product of the transmit and receive sensitivities, which are essentially identical at 1.5 T. In a second experiment, the metasurface performance was evaluated under more realistic scanning conditions using the body coil to transmit and a small (10 cm diameter) surface coil for receive. One surface coil was placed in an identical position above each wrist, with the metasurface placed below the right wrist. The signal-to-noise ratio (SNR) enhancement was measured as the ratio between the average value of the signal in the right wrist divided by that in the left.

3. Results

3.1. Electromagnetic simulations

Electromagnetic simulations of the metasurface are shown in Fig. 1. The metasurface supports a set of eigenmodes in the frequency range of the first Fabry-Perot regime. These eigenmodes are the result of the splitting of the original resonance frequency into several bands associated with the high coupling between the resonant wires, which are spaced apart by much less than one wavelength [14–16]. Each eigenmode can be characterized by its penetration depth and for all eigenmodes the magnetic field is concentrated in the central part of the metasurface while the electric field is maximum at its ends. In the current design, the metasurface was tuned to the eigenmode that has the highest penetration depth [11]. Fig. 1(c) shows that for this eigenmode of the metasurface the highest magnetic field is localized in the center of the metasurface (blue curve), and the electric field is confined near the ends of the wires (red curve). Compared to the setup described previously [11] the wires are placed much closer to the top part of the box to maximize the coupling with the subject who is positioned directly on top of the structure. Fig. 1(b) shows approximately a 300 kHz downward shift in frequency when a load with realistic loss is placed directly on top.

Fig. 2 shows the simulated B_1^+ maps for the human voxel model inside a birdcage body coil without (a) and with (b) the metasurface placed under the wrist. All simulations were normalized to 1 W accepted power. Comparing Fig. 2(a) and (b) the metasurface significantly enhances the B_1^+ field due to the coupling of the excitation field with the lowest frequency metasurface eigenmode: the increase of the B_1^+ in the imaging region-of-interest is a factor of 3.6. Of course, as with all surface elements, the magnetic field decreases with distance from the metasurface [Fig. 2(b)].

Fig. 2(c) and (d) shows the corresponding numerical SAR simulations without (c) and with (d) the metasurface. It should be noted that, in order to accommodate the metasurface, the body model is offset approximately 5 cm in the left–right direction, and this accounts for the asymmetry in the SAR maps. For 1 W accepted power for the cases without and with the metasurface, the maximum SAR values are 0.15 and 0.13 W/kg, respectively. There is a slight spatial redistribution of the SAR within the wrist below the metasurface.

3.2. In vivo results

Fig. 3 shows photographs of the *in vivo* setup and the metasurface. Volunteers were placed such that the wrist was positioned above the center of the metasurface while the other wrist was placed on top of an equivalently-sized sandbag. As mentioned above, the volunteer was offset slightly in the left–right direction to accommodate the metasurface.

As described in the methods section, images of the wrist were acquired with and without the metasurface using the body coil in both transmit and receive mode. The average increase in SNR was a factor of 11, corresponding to an increase in transmit efficiency of a factor of 3.3, slightly less than that obtained from electromagnetic simulations. Fig. 4 shows low tip angle gradient echo scans of the human wrist using the more realistic situation of body coil transmit and surface coil receive. An SNR improvement of a factor of 4.4 was measured in the wrist placed above the metasurface compared to the other wrist. Since this SNR increase is slightly higher than that of the transmit efficiency, one can conclude that the receive sensitivity of the surface coil is also improved due to the presence of the metasurface eigenmode, despite the presence

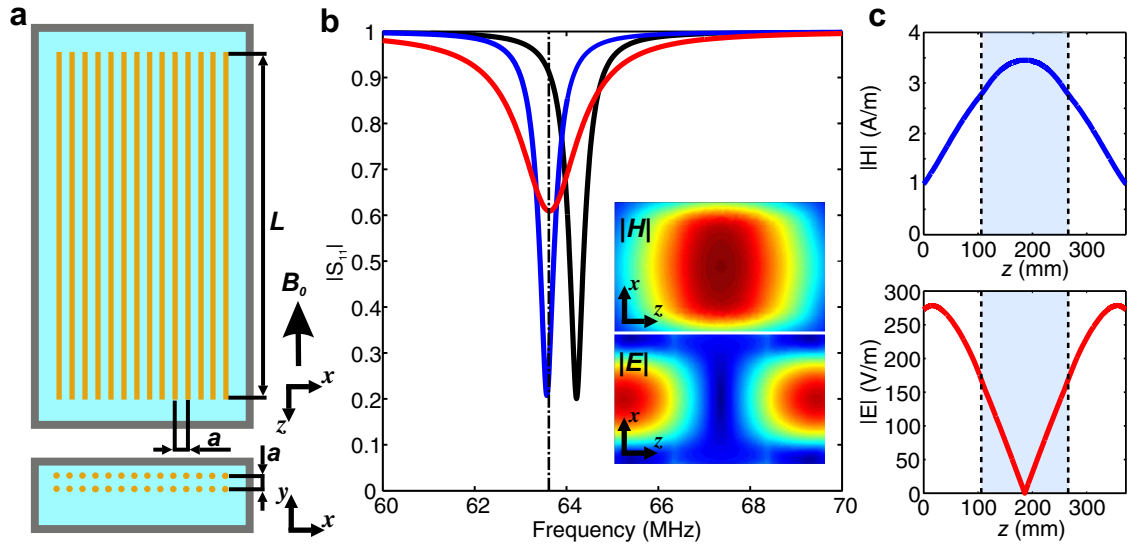

Fig. 1. Schematic illustration of the geometry of the wire metasurface: an array of 14 × 2 of parallel brass wires with $L = 37.2$ cm and $a = 1$ cm. (b) Numerical simulation results of the reflection coefficient ($|S_{11}|$) of a small untuned antenna placed below the metasurface. The black curve corresponds to the case of the unloaded metasurface, the blue curve to the case with the low loss phantom, and the red curve to the phantom with tissue mimicking conductivity. The dash-dot line indicates a frequency of 63.8 MHz. The insets illustrate numerically calculated magnetic ($|H|$) and electric ($|E|$) fields distributions in the region-of-interest at the resonance frequency. The color bar range of the H-field is 0 to 4 A/m and of the E-field is 0 to 300 V/m. (c) Numerically calculated magnetic (top panel) and electric (bottom panel) near-field profiles of the metasurface eigenmode with a highest penetration depth along the z-axis. Light blue shaded area and black dashed lines correspond the region-of-interest used for imaging. (For interpretation of the references to colour in this figure legend, the reader is referred to the web version of this article.)

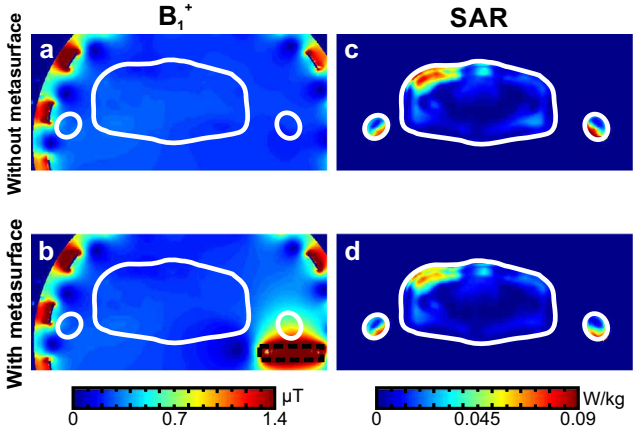

Fig. 2. Numerical simulation results of the B_1^+ and SAR (10 g) for a human voxel model placed inside the birdcage body coil. The calculated B_1^+ and SAR (10 g) maps without (a), (c) and with (b), (d) the metasurface for 1 W of accepted power. The white lines indicate the body outline in the transverse plane. The black dashed lines in (b) show the boundaries of the metasurface. Note that the body is positioned approximately 5 cm off-center in the left/right direction to accommodate the metasurface.

of some coupling between these two elements, and therefore some detuning of the receive coil.

4. Discussion and conclusion

The vast majority of clinical MRI scans use a body coil for transmission. While this allows homogeneous excitation over all body parts at a field strength of 1.5 T, it is naturally quite inefficient for imaging relatively small regions of the body such as the extremities. Although SAR is not typically a limiting factor at 1.5 T, it does become an issue when patients with metallic implants have to be scanned. In this case the local SAR limits must be reduced significantly, even if the body part being imaged does not correspond spatially to a region of high SAR. In this case it would be highly advantageous to be able to increase the local transmit efficiency close to the imaging region-of-interest since the overall power, and therefore SAR delivered to the patient can be decreased while maintaining optimum image quality.

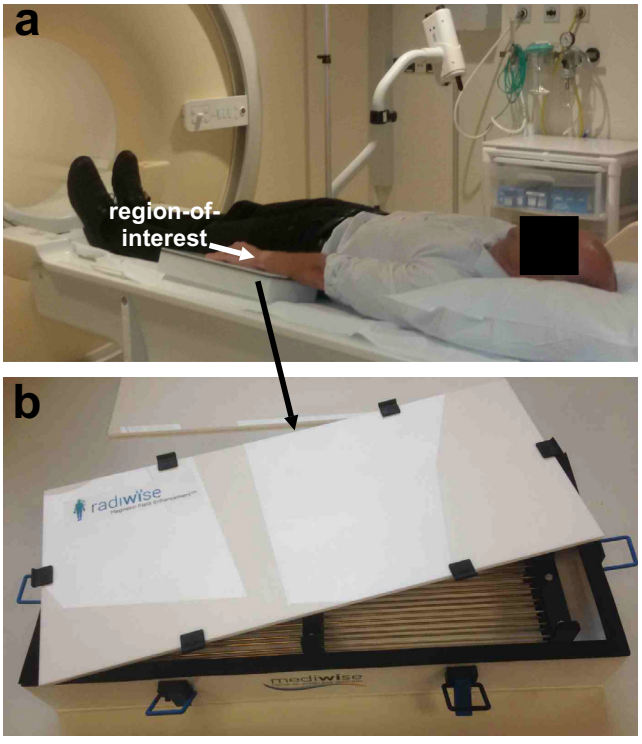

Fig. 3. Photographs of the *in vivo* setup (a) and metasurface (b). The metasurface was placed below the wrist of the volunteer. The brass wires are positioned inside the acrylic box which was filled with distilled water and sealed.

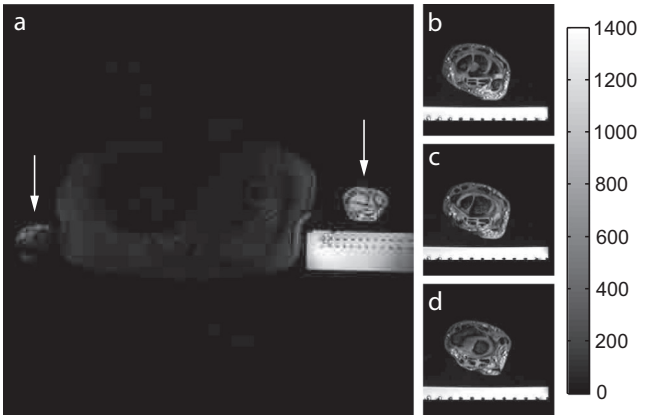

Fig. 4. Low tip angle gradient echo images of the wrist using body coil transmit and surface coils placed above each wrist for signal reception. (a) Enhancement of the signal in the wrist placed above the metasurface (right) compared to the wrist placed on top of a sandbag (left). White arrows indicate the two wrists. (b), (c), (d) High-resolution images from a multi-slice data set of the wrist placed on top of the metasurface with field-of-view = 120 × 120 mm.

Results presented in this paper demonstrate proof-of-principle experiments in the form of *in vivo* scans using a metasurface for local enhancement of the RF magnetic field in the region-of-interest under clinical scanning conditions. This metasurface can be considered as a wireless coil that redistributes electromagnetic fields and increases the local transmit efficiency in the area of interest. As such it operates in a very similar way to inductively-coupled wireless local coils [17,18], and indeed the mode structure is related to that of a low-pass planar "ladder" coil, albeit with the advantage of more flexible and intrinsically symmetric tuning via the dielectric rather than a large number of lumped element capacitors.

In its present form the metasurface clearly needs several improvements in design to increase its practical functionality. Future designs might incorporate ceramic substrates with a higher permittivity that would allow the metasurface to be made thinner. It would also be advantageous to be able to tune the spectrally eigenmode during transmission, and detune it during signal reception to remove any coupling effects with the receive coil array: this could potentially be achieved with the aid of different switchable electronic components as has been shown for nonlinear and tunable metamaterials [19,20]. It is also important to model the situation in which a body part is located in the area of strong electric field produced by coupling of the body coil to the metasurface in terms of the local SAR. The trade-off between the reduced power transmitted by the body coil, and the unevenly distributed electric field arising from the metasurface should be evaluated on a case-by-case basis, although we anticipate that for the vast majority of cases the maximum local SAR will be lower using the metasurface due to the overall increase in transmit efficiency. Finally, flexible metasurfaces based on the concept proposed for 7 T MRI [13] can be useful for specific applications where the structure is required to conform to the torso or head, and locally enhances the RF magnetic field in the region-of-interest. In contrast, in order to obtain homogeneous enhancement in the whole area a volumetric or semi-volumetric design [21] should be designed.

Acknowledgments

The authors are grateful to Rita Schmidt of Leiden University Medical Center, Shimul Chandra Saha, Ioannis Sotiriou and George Palikaras of Medical Wireless Sensing Ltd. The numerical calculations were supported by the Russian Science Foundation (Project No. 15-19-20054). Experimental studies were supported by the Ministry of Education and Science of the Russian Federation (Zadanie No. 3.2465.2017/4.6) and partially by the European Research Council Advanced Grant number 670629 (A.W.) and Medical Wireless Sensing Ltd.

References

[1] S. Nazarian, R. Beinart, H. Halperin, Magnetic resonance imaging and implantable devices, Circ. Arrhythm. Electrophysiol. 6 (2013) 419–428, https://doi.org/10.1161/CIRCEP.113.000116.
[2] Z. Yu, X. Xin, C. Collins, Potential for high-permittivity materials to reduce local SAR at a pacemaker lead tip during MRI of the head with a body transmit coil at 3 T, Magn. Reson. Med. 78 (2017) 383–386, https://doi.org/10.1002/mrm.26344.
[3] W. Brink, A. Webb, High permittivity pads reduce specific absorption rate, improve B1 homogeneity, and increase contrast-to-noise ratio for functional cardiac MRI at 3 T, Magn. Reson. Med. 71 (2014) 1632–1640, https://doi.org/10.1002/mrm.24778.
[4] A. Neves, L. Leroi, Z. Raolison, N. Cochinaire, T. Letertre, R. Abdeddaim, S. Enoch, J. Wenger, J. Berthelot, A. Adenot-Engelvin, N. Mallejac, F. Mauconduit, A. Vignaud, P. Sabouroux, Compressed perovskite aqueous mixtures near their phase transitions show very high permittivities: New prospects for high-field MRI dielectric shimming, Magn. Reson. Med. (2017), https://doi.org/10.1002/mrm.26771.
[5] N. Engheta, R. Ziolkowski, Metamaterials: Physics and Engineering Explorations, Wiley-IEEE Press, Piscataway, NJ, 2006.
[6] C. Holloway, E. Kuester, J. Gordon, J. O'Hara, J. Booth, D. Smith, An overview of the theory and applications of metasurfaces: The two-dimensional equivalents of metamaterials, IEEE Antennas Propag. Mag. 54 (2012) 10–35, https://doi.org/10.1002/mrm.1910390317.
[7] M. Wiltshire, J. Pendry, I. Young, D. Larkman, D. Gilderdale, J. Hajnal, Microstructured magnetic materials for RF flux guides in magnetic resonance imaging, Science 291 (2001) 849–851, https://doi.org/10.1126/science.291.5505.849.
[8] X. Radu, D. Garray, C. Craeye, Toward a wire medium endoscope for MRI imaging, Metamaterials 3 (2009) 90–99, https://doi.org/10.1016/j.jmr.2009.12.005.
[9] M. Freire, L. Jelinek, R. Marques, M. Lapine, On the applications of μ_r=-1 metamaterial lenses for magnetic resonance imaging, J. Magn. Reson. 203 (2010) 81–90, https://doi.org/10.1016/j.jmr.2009.12.005.
[10] R. Syms, T. Floume, I. Young, L. Solymar, M. Rea, Flexible magnetoinductive ring MRI detector: Design for invariant nearest-neighbour coupling, Metamaterials 4 (2010) 1–14, https://doi.org/10.1016/j.metmat.2009.12.001.
[11] A. Slobozhanyuk, A. Poddubny, A. Raaijmakers, C. van den Berg, A. Kozachenko, I. Dubrovina, I. Melchakova, Y. Kivshar, P. Belov, Enhancement of magnetic resonance imaging with metasurfaces, Adv. Mater. 28 (2016) 1832–1838, https://doi.org/10.1002/adma.201504270.
[12] C. Jouvaud, R. Abdeddaim, B. Larrat, J. de Rosny, Volume coil based on hybridized resonators for magnetic resonance imaging, Appl. Phys. Lett. 108 (1-5) (2016) 023503, https://doi.org/10.1063/1.4939784.
[13] R. Schmidt, A. Slobozhanyuk, P. Belov, A. Webb, Flexible and compact hybrid metasurfaces for enhanced ultra high field in vivo magnetic resonance imaging, Sci. Rep. 7 (2017) 1678, https://doi.org/10.1038/s41598-017-01932-9.
[14] F. Lemoult, G. Lerosey, J. Rosny, M. Fink, Resonant metalenses for breaking the diffraction barrier, Phys. Rev. Lett. 104 (2010) 203901, https://doi.org/10.1103/PhysRevLett.104.203901.
[15] F. Lemoult, M. Fink, G. Lerosey, Revisiting the wire medium: an ideal resonant metalens, Waves Random Complex Medium 21 (2011) 591–613, https://doi.org/10.1080/17455030.2011.611836.
[16] A. Slobozhanyuk, A. Poddubny, A. Krasnokand, P. Belov, Magnetic Purcell factor in wire metamaterials, Appl. Phys. Lett. 104 (2014) 161105, https://doi.org/10.1063/1.4872163.
[17] H. Shigehiro, S. Tomohiro, T. Hiroshi, M. Shuichi, K. Yuki, M. Yuichirou, N. Takashi, K. Kagayaki, Application of inductively coupled wireless radio frequency probe to knee joint in magnetic resonance image, J. Syst. Cybern. Informatics 7 (5) (2009) 6–10.
[18] S. Bulumulla, E. Fiveland, K. Park, T. Foo, C. Hardy, Inductively coupled wireless RF coil arrays, Magn. Reson. Imaging 33 (3) (2015) 351–357, https://doi.org/10.1016/j.mri.2014.12.004.
[19] A. Slobozhanyuk, P. Kapitanova, D. Filonov, D. Powell, I. Shadrivov, M. Lapine, P. Belov, R. McPhedran, Y. Kivshar, Nonlinear interaction of meta-atoms through optical coupling, Appl. Phys. Lett. 104 (2014) 014104, https://doi.org/10.1063/1.4861388.
[20] M. Lapine, I. Shadrivov, Y. Kivshar, Colloquium: Nonlinear metamaterials, Rev. Mod. Phys. 86 (2014) 1093, https://doi.org/10.1103/RevModPhys.86.1093.
[21] R. Schmidt, W. Teeuwisse, A. Webb, Quadrature operation of segmented dielectric resonators facilitated with metallic connectors, Magn. Reson. Med. 77 (2017) 2431–2437, https://doi.org/10.1002/mrm.26301.